Chiral dynamics of three-mode non-Hermitian systems with a periodical driving

La-Tai You,[1] Yu-Jia Gao,[1] Guang-Tao Wang,[2] and Gong-Ping Zheng[1,3,4,*]

[1]*College of Physics and Electronic Information Engineering, Qinghai Normal University, Xining, Qinghai 810016, China*
[2]*College of Physics, Henan Normal University, Xinxiang, Henan 453007, China*
[3]*Lanzhou Center for Theoretical Physics, Key Laboratory of Theoretical Physics of Gansu Province,*
Lanzhou University, Lanzhou, Gansu 730000, China
[4]*Academy of Plateau Science and Sustainability, Xining, Qinghai 810016, China*

The chiral dynamics of three-mode non-Hermitian systems with a periodical driving are studied. An exact chiral behavior of the relative phases of the final states after encircling with opposite directions in parameter space is obtained analytically with the solutions of the dynamical equations. It is shown that the relative phases of the evolution states are opposite numbers for the clockwise and counterclockwise loops of the driving parameters. But the density distributions have no chirality during the evolution. We examine the dynamical behavior by a numerical simulation of the evolution equations, which agrees well with our analytical predictions for the adiabatic evolution. The final density distributions are found to be independent of initial states and always the same for the clockwise and counterclockwise encircling, while in most examples discussed in the literature the amplitudes show a nonsymmetric behavior when the parameter space circles are in opposite directions. It is also found that the dynamical behavior is steady for the long-time evolution. We attribute the results to the special symmetry of the model, which might encourage others to work on physical realizations of the model.

I. INTRODUCTION

Non-Hermitian physics, which studies the open systems with dissipative energy, particle, and information, has become a very active field in both experimental and theoretical research (see the review papers in Refs. [1–5]). Many exotic phenomena were found, which are absent in the traditional Hermitian physics, such as the parity-time-symmetry ($\mathcal{PT}$) and anti-$\mathcal{PT}$ systems [6–33], the non-Hermitian skin effects [34–58], etc.

The dynamics of non-Hermitian systems have attracted increasing attention. A dissipative system is described by the non-Hermitian Hamiltonian. For the time-independent Hamiltonian, there are two fundamental features of non-Hermitian dynamics. In some parameter region, the eigenenergies of the non-Hermitian Hamiltonian can be real due to the balance between the gain and loss. In such a case, the dynamics of a dissipative system behaves as a conservative system described by the Hermitian Hamiltonian. The other feature is the selection of a state which dominates the final density distribution after a long-time evolution. The reason is that the eigenstate with a maximum nonzero imaginary part will decrease very slowly or increase very rapidly among all the eigenstates, which will be selected as the final state after a long-time evolution [59,60].

For the time-dependent non-Hermitian Hamiltonian, the dynamic is more complicated. A dramatic phenomenon is the appearance of chirality in non-Hermitian dynamics with

periodical driving [61–64]. Starting from the same point in the driving-parameter space, the final states will be converted at the same end point of one-period evolution for the clockwise (CW) and counterclockwise (CCW) circles. The chiral dynamics has been studied extensively in a two-mode non-Hermitian system, especially with regard to the effects of encircling exception points (EPs) on the chiral dynamics [65–87]. Although there are some studies on the properties of three-mode non-Hermitian systems [88–93], the chiral dynamics of a three-mode non-Hermitian system has not been extensively studied and is yet to be investigated. Reference [89] contains an example, which can be explained by a three-mode non-Hermitian model. The nonadiabatic population transfer was studied. The chiral dynamics of a three-mode waveguide system has also been studied in Ref. [92], when dynamically encircling EPs. Their investigation focused on the final density distributions of the encircling and the chiral behavior of the density distributions was found. In this paper, we study a three-mode non-Hermitian model with a certain symmetry. We find that the final density distributions are always the same for the CW and CCW encircling, namely, no chiral behavior for the final density distributions. Meanwhile, we observe an exact chiral behavior for the relative phases of the final states, which are supported by both our analytical results and numerical simulation of the dynamical equations. We attribute the results to the special symmetry of the model, which might encourage others to work on the physical realizations of the model.

The paper is organized as follows: In Sec. II, we introduce the model of a three-mode non-Hermitian system with a periodical driving. In Sec. III, the chirality of the evolution

---

*Contact author: zhenggongping@aliyun.com

equations is observed analytically. We solve numerically the evolution equations and confirm the chiral behavior of the three-mode non-Hermitian systems in Sec. IV. Finally, we summarize our results and give some remarks in Sec. V.

II. MODEL OF THREE-MODE NON-HERMITIAN SYSTEMS

We consider a three-mode non-Hermitian system driven by a periodical force with the following Hamiltonian [3],

$$\hat{H} = \begin{pmatrix} ig + \delta & -1 & 0 \\ -1 & 0 & -1 \\ 0 & -1 & -ig - \delta \end{pmatrix}, \quad (1)$$

where the dimensionless parameters g and δ are both real and time dependent.

The eigenvalues of the Hamiltonian (1) can be obtained as

$$\lambda_0 = 0, \quad \lambda_\pm = \pm\sqrt{2 - Z^2}, \quad (2)$$

where $Z \equiv g - i\delta$. The corresponding right eigenstates are

$$|\lambda_0\rangle = \frac{1}{\sqrt{n_0}}(1, iZ, -1)^T,$$

$$|\lambda_\pm\rangle = \frac{1}{\sqrt{n_\pm}}\left(\frac{1}{iZ \mp \sqrt{2 - Z^2}}, 1, \frac{1}{-iZ \mp \sqrt{2 - Z^2}}\right)^T, \quad (3)$$

where T is for the transpose and $n_0 = n_\pm = 2 - Z^2$ are the normalization constants. We emphasize here that the instantaneous eigenvalues and corresponding instantaneous eigenstates are as given for the entire time during the evolution. For the time-independent eigenvalue λ_0, the instantaneous eigenstate $|\lambda_0\rangle$ is also time dependent.

The eigenstates of the Hermitian-conjugate Hamiltonian $\hat{H}^\dagger$ can also be obtained as

$$|\chi_0\rangle = \frac{1}{\sqrt{n_0^*}}(1, -iZ^*, -1)^T,$$

$$|\chi_\pm\rangle = \frac{1}{\sqrt{n_\pm^*}}\left(\frac{1}{-iZ^* \mp \sqrt{2 - Z^{*2}}}, 1, \frac{1}{iZ^* \mp \sqrt{2 - Z^{*2}}}\right)^T, \quad (4)$$

with the eigenvalues

$$\chi_0 = 0, \quad \chi_\pm = \pm\sqrt{2 - Z^{*2}} = \lambda_\pm^*. \quad (5)$$

$\langle\chi_{0,\pm}| = |\chi_{0,\pm}\rangle^\dagger$ describe the so-called left eigenstates. The two sets of eigenstates satisfy the biorthogonal relation $\langle\chi_i|\lambda_j\rangle = \delta_{ij}$ [59], where $i, j = 0, \pm$. A couple of left and right eigenstates with the complex-conjugate eigenvalues are normalized. For the other cases, they are orthogonal. Because the symmetry $\hat{H}^T = \hat{H}$ of the Hamiltonian (1), the components of the biorthogonal left eigenstates $\langle\chi_{0,\pm}|$ are the same as those of the right eigenstates $|\lambda_{0,\pm}\rangle$.

For the particular parameter values $Z = \pm\sqrt{2}$, we arrive at the third-order exception points (EPs),

$$\lambda_0 = \lambda_\pm = 0, \quad (6)$$

with

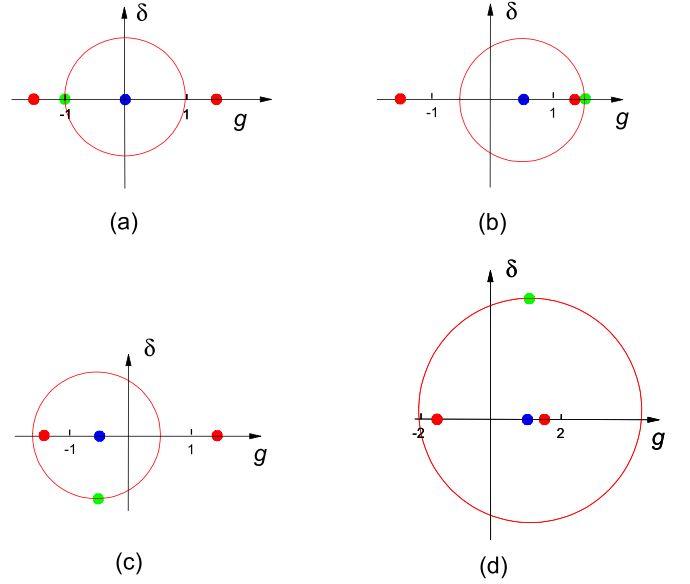$$|\lambda_{0,\pm}\rangle = (-i, \sqrt{2}, i)^T. \quad (7)$$

FIG. 1. Schematic showing the relation among the EPs, the starting points, and the central points of the loops in the dimensionless (g, δ) space. The red, green, and blue dots are for the EPs, the starting points, and the central points of the loops, respectively.

The EPs locate at $Z = \pm\sqrt{2}$, namely, $g = \pm\sqrt{2}$ and $\delta = 0$. It is emphasized that the EPs $(\pm\sqrt{2}, 0)$ in the (g, δ) space are time independent.

We assume the dependence of the driving parameters on time $g = g_0 - \rho\cos(\gamma t)$ and $\delta = \rho\sin(\gamma t)$. γ measures the driving frequency and in this paper we pay special attention to the adiabatic evolution, namely, $\gamma \to 0$. The parameters will return to the starting point after one period $T = 2\pi\gamma^{-1}$ in the (g, δ) space. This loop, centered at g_0, has a radius of ρ. Without loss of generality, we consider the case where $\rho > 0$. $\gamma > 0$ ($\gamma < 0$) describes the CW (CCW) circle.

The number of EPs that the loop encircles depends on the parameters g_0 and ρ. There are four cases as follows: (1) no EP is encircled, for example, $g_0 = 0$ and $\rho < \sqrt{2}$; see Fig. 1(a); (2) the right EP is encircled, for example, $0 < g_0 < \sqrt{2}$ and $\sqrt{2} - g_0 < \rho < g_0 + \sqrt{2}$; see Fig. 1(b); (3) the left EP is encircled, for example, $-\sqrt{2} < g_0 < 0$ and $\sqrt{2} + g_0 < \rho < \sqrt{2} - g_0$; see Fig. 1(c); and (4) two EPs are encircled, for example, $0 < g_0 < \sqrt{2}$ and $g_0 + \sqrt{2} < \rho$; see Fig. 1(d).

In Fig. 1, we schematically show the relation among the EPs, the starting points, and the central points of the loops in the (g, δ) space.

III. CHIRALITY OF THE DYNAMICAL EQUATIONS

The dynamical behavior can be described by the Schrödinger equation

$$i\frac{d}{dt}\Psi = \hat{H}\Psi, \quad (8)$$

where $\Psi = (\psi_1, \psi_2, \psi_3)^T$ and we have taken $\hbar = 1$.

The general dynamics of an open quantum system should be governed by the Lindblad master equation [94–96], which contains the quantum jump term that is absent in the above

Schrödinger equation based on the non-Hermitian Hamiltonian. The general Lindblad master equation of the density matrix can describe the dynamics of mixed states, while the above Schrödinger equation is only suitable for the pure state, which is the case we considered in this paper.

For the Hamiltonian (1), we obtain

$$i\dot{\psi}_1^{\mathrm{CW}} = i(g_0 - \rho e^{i\gamma t})\psi_1^{\mathrm{CW}} - \psi_2^{\mathrm{CW}},$$
$$i\dot{\psi}_2^{\mathrm{CW}} = -\psi_1^{\mathrm{CW}} - \psi_3^{\mathrm{CW}},$$
$$i\dot{\psi}_3^{\mathrm{CW}} = -\psi_2^{\mathrm{CW}} - i(g_0 - \rho e^{i\gamma t})\psi_3^{\mathrm{CW}}, \quad (9)$$

for the three modes of the CW encircling of the parameters. For the CCW case, namely, $\gamma \to -\gamma$, we have

$$i\dot{\psi}_1^{\mathrm{CCW}} = i(g_0 - \rho e^{-i\gamma t})\psi_1^{\mathrm{CCW}} - \psi_2^{\mathrm{CCW}},$$
$$i\dot{\psi}_2^{\mathrm{CCW}} = -\psi_1^{\mathrm{CCW}} - \psi_3^{\mathrm{CCW}},$$
$$i\dot{\psi}_3^{\mathrm{CCW}} = -\psi_2^{\mathrm{CCW}} - i(g_0 - \rho e^{-i\gamma t})\psi_3^{\mathrm{CCW}}. \quad (10)$$

By taking the complex conjugation of the above equations, we obtain

$$i(\dot{\psi}_1^{\mathrm{CCW}})^* = i(g_0 - \rho e^{i\gamma t})(\psi_1^{\mathrm{CCW}})^* + (\psi_2^{\mathrm{CCW}})^*,$$
$$i(\dot{\psi}_2^{\mathrm{CCW}})^* = (\psi_1^{\mathrm{CCW}})^* + (\psi_3^{\mathrm{CCW}})^*,$$
$$i(\dot{\psi}_3^{\mathrm{CCW}})^* = (\psi_2^{\mathrm{CCW}})^* - i(g_0 - \rho e^{i\gamma t})(\psi_3^{\mathrm{CCW}})^*, \quad (11)$$

namely,

$$i(-\dot{\psi}_1^{\mathrm{CCW}})^* = i(g_0 - \rho e^{i\gamma t})(-\psi_1^{\mathrm{CCW}})^* - (\psi_2^{\mathrm{CCW}})^*,$$
$$i(\dot{\psi}_2^{\mathrm{CCW}})^* = -(-\psi_1^{\mathrm{CCW}})^* - (-\psi_3^{\mathrm{CCW}})^*,$$
$$i(-\dot{\psi}_3^{\mathrm{CCW}})^* = -(\psi_2^{\mathrm{CCW}})^* - i(g_0 - \rho e^{i\gamma t})(-\psi_3^{\mathrm{CCW}})^*. \quad (12)$$

Comparing Eqs. (12) with Eqs. (9), the CCW evolution can be easily obtained by the replacement of $(\psi_1^{\mathrm{CW}}, \psi_2^{\mathrm{CW}}, \psi_3^{\mathrm{CW}}) \to [-(\psi_1^{\mathrm{CCW}})^*, (\psi_2^{\mathrm{CCW}})^*, -(\psi_3^{\mathrm{CCW}})^*]$. It means that the density distributions are the same for the CW and CCW loops, namely, $|\psi_i^{\mathrm{CW}}|^2 = |\psi_i^{\mathrm{CCW}}|^2$. But the phases of the evolution states are different for the CW and CCW encircling, more exactly speaking, $\arg(\psi_1^{\mathrm{CCW}}, \psi_2^{\mathrm{CCW}}, \psi_3^{\mathrm{CCW}}) = (\pi - \arg\psi_1^{\mathrm{CW}}, -\arg\psi_2^{\mathrm{CW}}, \pi - \arg\psi_3^{\mathrm{CW}})$. To show the chiral behavior of the system, we introduce the relative phase $\theta_{31} \equiv \arg(\psi_3) - \arg(\psi_1)$. It is obvious that $\arg(\psi_3^{\mathrm{CCW}}) - \arg(\psi_1^{\mathrm{CCW}}) = -[\arg(\psi_3^{\mathrm{CW}}) - \arg(\psi_1^{\mathrm{CW}})]$, namely, $\theta_{31}^{\mathrm{CCW}} = -\theta_{31}^{\mathrm{CW}}$.

We emphasize here that the exact chiral behavior is obtained from the symmetry of the differential equations, which describes the instantaneous behavior of the evolution states at any evolution time t. For the long-time evolution, the final state may be not. We will examine the dynamical behavior by numerical simulation of the evolution equations.

The dynamical behavior of the left eigenstate can be described by the Schrödinger equation with the driving Hamiltonian $\hat{H}^\dagger$,

$$i\frac{d}{dt}\Theta = \hat{H}^\dagger\Theta, \quad (13)$$

where $\Theta = (\Theta_1, \Theta_2, \Theta_3)^T$ and $\Theta^\dagger$ describes the left eigenstate. For the Hamiltonian (1), we can obtain a similar result of $\arg(\Theta_1^{\mathrm{CCW}}, \Theta_2^{\mathrm{CCW}}, \Theta_3^{\mathrm{CCW}}) =$

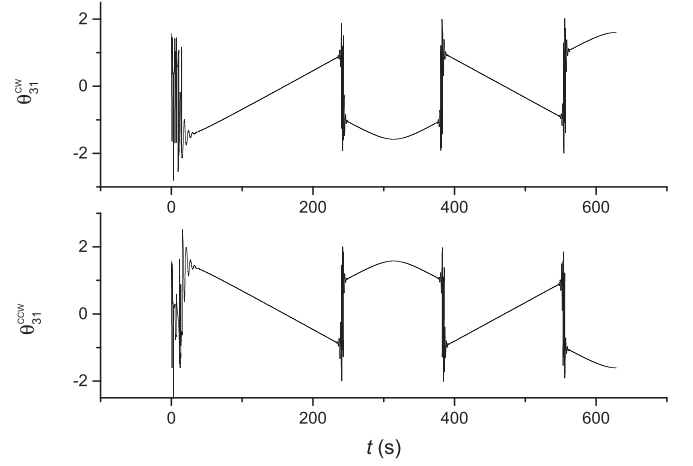

FIG. 2. Real-time evolution of the relative phase θ_{31} for one period T. The top is for the CW encircling and the bottom is for the CCW encircling. The initial state is the instantaneous eigenstate $|\lambda_+\rangle$ at $t = 0$. The dimensionless parameters are $g_0 = 0$, $\rho = 1$. The driving frequency is $|\gamma| = 0.01$ Hz for the CW and CCW loops.

$(\pi - \arg\Theta_1^{\mathrm{CW}}, -\arg\Theta_2^{\mathrm{CW}}, \pi - \arg\Theta_3^{\mathrm{CW}})$, namely, $\arg(\Theta_3^{\mathrm{CCW}}) - \arg(\Theta_1^{\mathrm{CCW}}) = -[\arg(\Theta_3^{\mathrm{CW}}) - \arg(\Theta_1^{\mathrm{CW}})]$. For the numerical simulation, we have similar results for the left eigenstates.

IV. CHIRAL DYNAMICS WITH THE NUMERICAL SIMULATION

To confirm the dynamical behavior of the system, we do the numerical simulation of the evolution equation (8). We find that for all cases the final density distributions after the evolution of one period T are independent of the choice of the initial states. We have chosen some quite different initial states, such as the instantaneous eigenstates $|\lambda_0\rangle$ and $|\lambda_\pm\rangle$ at $t = 0$, even the state $(1, 1, 1)^T$, and other random initial distributions.

Our numerical simulations confirm that the final density distributions are indeed the same for the CW and CCW encircling, namely, no chiral behavior. This is a clear difference from other systems, because in most examples discussed in the literature the amplitudes show a nonsymmetric behavior when the parameter space loops are in opposite directions. We attribute the result to the special symmetry of the matrix model, namely, $\hat{H}^T = \hat{H}$.

But the chiral evolution can occur for the relative phases. Next, we show the real-time evolution of the relative phases θ_{31} for both the CW and CCW encircling. In Fig. 2, it is for the loop with no EP enclosed, corresponding to that in Fig. 1(a). The initial state is set as the instantaneous eigenstate $|\lambda_+\rangle$ at $t = 0$. In Fig. 3, it is for the loop with the right EP enclosed, corresponding to that in Fig. 1(b). The starting point locates at the right of the loop, corresponding to the driving parameters $g = g_0 - \rho\cos(\gamma t + \pi)$ and $\delta = \rho\sin(\gamma t + \pi)$ now. The initial state is set as the instantaneous eigenstate $|\lambda_-\rangle$ at the initial time. The chiral behavior can be seen clearly in the two figures, which agree well with our analytical predictions, namely, the relative phase $\theta_{31}^{\mathrm{CCW}} = -\theta_{31}^{\mathrm{CW}}$.
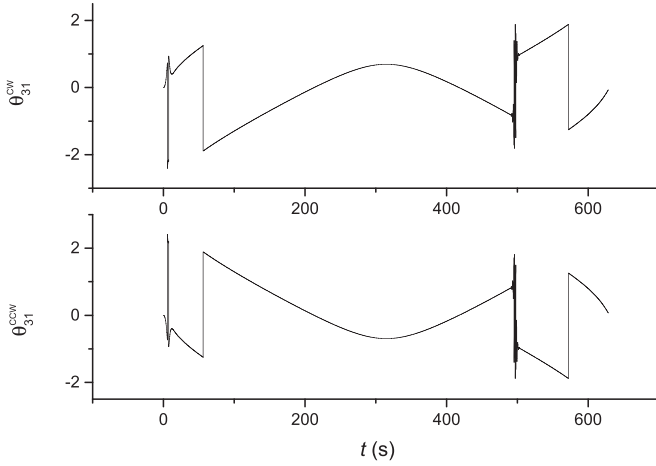
FIG. 3. Real-time evolution of the relative phase θ_{31} for one period T. The top is for the CW encircling and the bottom is for the CCW encircling. The initial state is the instantaneous eigenstate $|\lambda_-\rangle$ at $t = 0$. The dimensionless parameters are $g_0 = 0.5$, $\rho = 1$. The driving frequency is $|\gamma| = 0.01$ Hz for the CW and CCW loops.

FIG. 5. Real-time evolution of the relative phase θ_{31} for one period T. The top is for the CW encircling and the bottom is for the CCW encircling. The initial state is the instantaneous eigenstate $|\lambda_-\rangle$ at $t = 0$. The dimensionless parameters are $g_0 = -0.5$, $\rho = 1$. The driving frequency is $|\gamma| = 0.001$ Hz for the CW and CCW loops.

To examine the stability of the chirality, we have also simulated the dynamics for a long time. The result show that the chiral behavior of dynamics is steady for the long-time evolution. In Fig. 4, we show the double-period evolution of the relative phase θ_{31}. The parameters are the same as those in Fig. 2 except for the evolution time.

In Fig. 5, we show the loop with the left EP enclosed, corresponding to that in Fig. 1(c). The starting point locates at the bottom of the loop, now corresponding to the driving parameters $g = g_0 - \rho \cos(\gamma t - \pi/2)$ and $\delta = \rho \sin(\gamma t - \pi/2)$. The initial state is set as the instantaneous eigenstate $|\lambda_-\rangle$ at the initial time. In Fig. 6, we show the loop with two EP enclosed, corresponding to that in Fig. 1(d). The starting point locates at the top of the loop, now corresponding to the driven parameters $g = g_0 - \rho \cos(\gamma t + \pi/2)$ and $\delta = \rho \sin(\gamma t + \pi/2)$. The initial state is set as the instantaneous eigenstate $|\lambda_+\rangle$ at the initial time.

Obviously, the exact chiral behavior of the relative phases $\theta_{31}^{\text{CCW}} = -\theta_{31}^{\text{CW}}$ is absent now. We have simulated the dynamics with the same parameters of Figs. 5 and 6, except that the starting points locate on the g axis in the (g, δ) space, namely, the same starting points as those in Figs. 2 and 3. It shows the same chiral behavior as those in Figs. 2 and 3. So the disappearance of the exact chiral dynamics is due to the starting points not locating on the g axis in the parameter space. Although the exact chiral behavior of the relative phases $\theta_{31}^{\text{CCW}} = -\theta_{31}^{\text{CW}}$ is now absent, the relative phases are still different for the CW and CCW encircling. Then we can say that the chiral behavior still exist in such cases.

The final density distributions of Figs. 5 and 6 are still independent of the initial states and the same for the CW and CCW encircling, namely, there is no chiral behavior for the
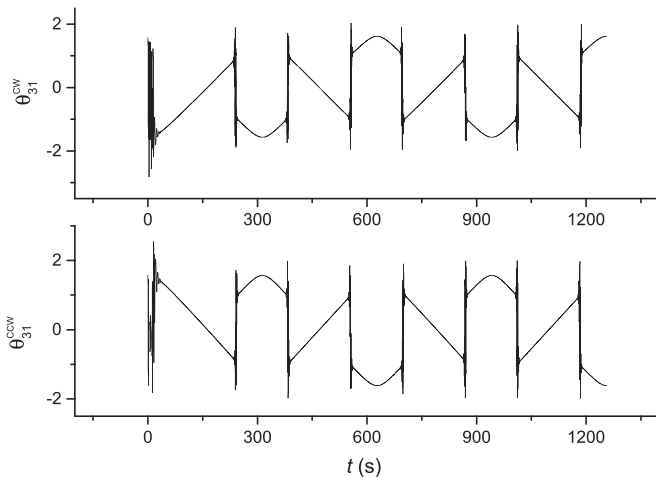

FIG. 4. Long-time evolution of the relative phase θ_{31} for two periods. The parameters are the same with those in Fig. 2 except for the evolution time.
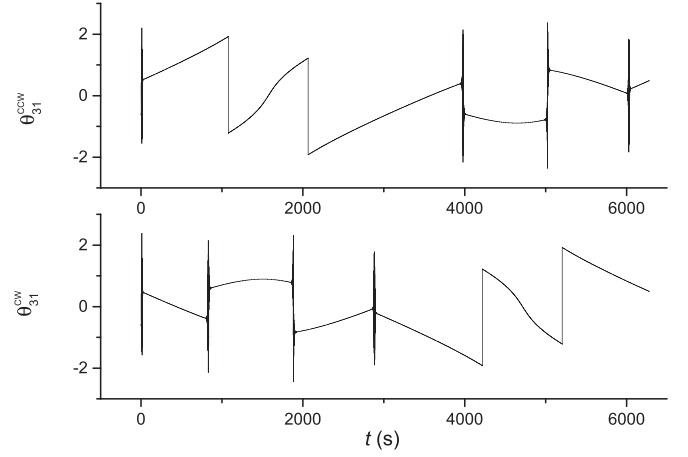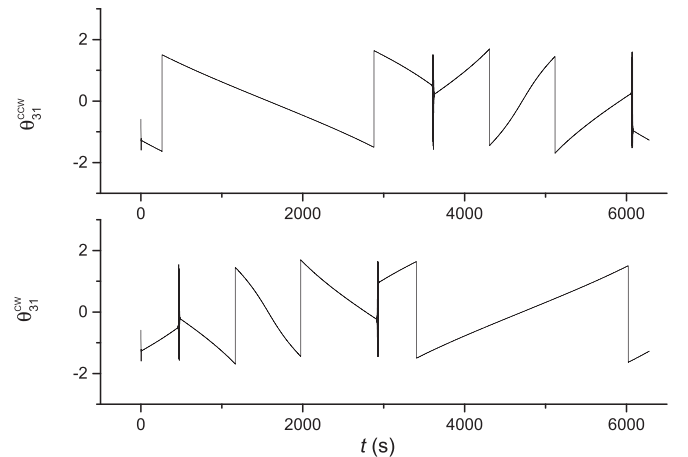

FIG. 6. Real-time evolution of the relative phase θ_{31} for one period T. The top is for the CW encircling and the bottom is for the CCW encircling. The initial state is the instantaneous eigenstate $|\lambda_+\rangle$ at $t = 0$. The dimensionless parameters are $g_0 = 1$, $\rho = 3$. The driving frequency is $|\gamma| = 0.001$ Hz for the CW and CCW loops.
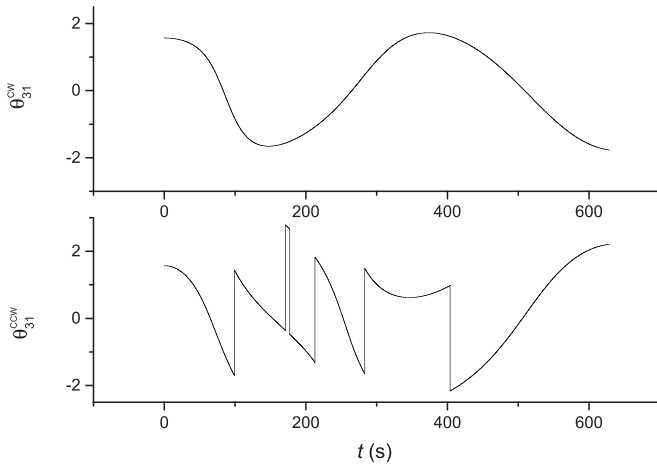
FIG. 7. Nonadiabatic evolution of the relative phase θ_{31} for one period T. The other parameters are the same as those in Fig. 2 except for the driving frequency γ, which is in units here.

density distributions, which still agrees with our analytical result. We emphasize that the adiabatic parameter γ of Figs. 5 and 6 is different than those of Figs. 2 and 3. If we take the same value of γ with those of Figs. 2 and 3, the final density distributions will be different. The same density distributions of the evolution states $|\psi_i^{\text{CW}}|^2 = |\psi_i^{\text{CCW}}|^2$ at any evolution time t are obtained from the symmetry of the differential equations, which describes the instantaneous behavior. For the long-time numerical simulation of the evolution equations, the final density distributions at the ending time of the loops may

not be the same. The long-time dynamics of the system is strongly affected by the adiabatic parameter γ.

V. CONCLUSION AND REMARKS

In summary, we have studied the dynamics of a symmetric three-mode non-Hermitian systems with a periodical driving. The exact chiralities of the dynamical equations are obtained analytically, which agree well with our numerical simulation of the adiabatic evolution, if the starting points are accurately chosen.

We have also done the nonadiabatic simulation of the same system. It is shown that the chirality will be absent and the final density distributions will be irregular. In Fig. 7, we show the dynamical behavior of the relative phase θ_{31} for the nonadiabatic evolution. The other parameters are the same as those in Fig. 2 except for the driving frequency γ, which measures the adiabaticity of evolution.

The chiral dynamics of three-mode waveguide system has been studied in Ref. [92], so our symmetric non-Hermitian model might be easier to be realized in optical waveguides. The chiral behavior $\theta_{31}^{\text{CCW}} = -\theta_{31}^{\text{CW}}$ of adiabatic evolution might be measured with *in situ* control of the encircling loop with a tunable external field [76].

[1] C. M. Bender, Making sense of non-Hermitian Hamiltonians, Rep. Prog. Phys. **70**, 947 (2007).

[2] R. El-Ganainy, G. M. Konstantinos, M. Khajavikhan, Z. H. Musslimani, S. Rotter, and D. N. Christodoulides, Non-Hermitian physics and *PT* symmetry, Nat. Phys. **14**, 11 (2018).

[3] Y. Ashida, Z. Gong, and M. Ueda, Non-Hermitian physics, Adv. Phys. **69**, 249 (2020).

[4] E. J. Bergholtz, J. C. Budich, and F. K. Kunst, Exceptional topology of non-Hermitian systems, Rev. Mod. Phys. **93**, 015005 (2021).

[5] K. Ding, C. Fang, and G. Ma, Non-Hermitian topology and exceptional-point geometries, Nat. Rev. Phys. **4**, 745 (2022).

[6] C. M. Bender and S. Boettcher, Real spectra in non-Hermitian Hamiltonians having $\mathcal{PT}$ symmetry, Phys. Rev. Lett. **80**, 5243 (1998).

[7] C. M. Bender, S. Boettcher, and P. N. Meisinger, $\mathcal{PT}$-symmetric quantum mechanics, J. Math. Phys. **40**, 2201 (1999).

[8] G. Lévai and M. Znojil, Systematic search for *PT*-symmetric potentials with real energy spectra, J. Phys. A: Math. Gen. **33**, 7165 (2000).

[9] C. M. Bender, D. C. Brody, and H. F. Jones, Complex extension of quantum mechanics, Phys. Rev. Lett. **89**, 270401 (2002).

[10] R. El-Ganainy, K. G. Makris, D. N. Christodoulides, and Z. H. Musslimani, Theory of coupled optical *PT*-symmetric structures, Opt. Lett. **32**, 2632 (2007).

[11] K. G. Makris, R. El-Ganainy, D. N. Christodoulides, and Z. H. Musslimani, Beam dynamics in $\mathcal{PT}$ symmetric optical lattices, Phys. Rev. Lett. **100**, 103904 (2008).

[12] Z. H. Musslimani, K. G. Makris, R. El-Ganainy, and D. N. Christodoulides, Optical solitons in $\mathcal{PT}$ periodic potentials, Phys. Rev. Lett. **100**, 030402 (2008).

[13] A. Guo, G. J. Salamo, D. Duchesne, R. Morandotti, M. Volatier-Ravat, V. Aimez, G. A. Siviloglou, and D. N. Christodoulides, Observation of $\mathcal{PT}$-symmetry breaking in complex optical potentials, Phys. Rev. Lett. **103**, 093902 (2009).

[14] S. Longhi, Bloch oscillations in complex crystals with $\mathcal{PT}$ symmetry, Phys. Rev. Lett. **103**, 123601 (2009).

[15] O. Bendix, R. Fleischmann, T. Kottos, and B. Shapiro, Exponentially fragile $\mathcal{PT}$ symmetry in lattices with localized eigenmodes, Phys. Rev. Lett. **103**, 030402 (2009).

[16] C. E. Rüter, G. M. Konstantinos, R. El-Ganainy, D. N. Christodoulides, M. Segev, and D. Kip, Observation of parity time symmetry in optics, Nat. Phys. **6**, 192 (2010).

[17] J. Schindler, A. Li, M. C. Zheng, F. M. Ellis, and T. Kottos, Experimental study of active *LRC* circuits with $\mathcal{PT}$ symmetries, Phys. Rev. A **84**, 040101(R) (2011).

[18] Z. Lin, H. Ramezani, T. Eichelkraut, T. Kottos, H. Cao, and D. N. Christodoulides, Unidirectional invisibility induced by $\mathcal{PT}$-symmetric periodic structures, Phys. Rev. Lett. **106**, 213901 (2011).

[19] A. Szameit, M. C. Rechtsman, O. Bahat-Treidel, and M. Segev, $\mathcal{PT}$-symmetry in honeycomb photonic lattices, Phys. Rev. A **84**, 021806(R) (2011).

[20] S. Bittner, B. Dietz, U. Günther, H. L. Harney, M. Miski-Oglu, A. Richter, and F. Schäfer, $\mathcal{PT}$ symmetry and spontaneous symmetry breaking in a microwave billiard, Phys. Rev. Lett. **108**, 024101 (2012).

[21] H. Ramezani, D. N. Christodoulides, V. Kovanis, I. Vitebskiy, and T. Kottos, $\mathcal{PT}$-symmetric Talbot effects, Phys. Rev. Lett. **109**, 033902 (2012).

[22] D. M. Jović, C. Denz, and M. R. Belić, Anderson localization of light in PT-symmetric optical lattices, Opt. Lett. **37**, 4455 (2012).

[23] A. Regensburger, C. Bersch, M.-A. Miri, G. Onishchukov, D. N. Christodoulides, and U. Peschel, Parity-time synthetic photonic lattices, Nature (London) **488**, 167 (2012).

[24] C. M. Bender, B. K. Berntson, D. Parker, and E. Samuel, Observation of PT phase transition in a simple mechanical system, Am. J. Phys. **81**, 173 (2013).

[25] X. Zhu, L. Feng, P. Zhang, X. Yin, and X. Zhang, One-way invisible cloak using parity-time symmetric transformation optics, Opt. Lett. **38**, 2821 (2013).

[26] N. Lazarides and G. P. Tsironis, Gain-driven discrete breathers in $\mathcal{PT}$-symmetric nonlinear metamaterials, Phys. Rev. Lett. **110**, 053901 (2013).

[27] L. Feng, Y. Xu, W. S. Fegadolli, M.-H. Lu, J. E. B. Oliveira, V. R. Almeida, Y.-F. Chen, and A. Scherer, Experimental demonstration of a unidirectional reflectionless parity-time metamaterial at optical frequencies, Nat. Mater. **12**, 108 (2013).

[28] R. Fleury, D. Sounas, and A. Alù, An invisible acoustic sensor based on parity-time symmetry, Nat. Commun. **6**, 5905 (2015).

[29] M. Kulishov, H. F. Jones, and B. Kress, Analysis of unidirectional non-paraxial invisibility of purely reflective PT-symmetric volume gratings, Opt. Express **23**, 18694 (2015).

[30] M. Wimmer, M.-A. Miri, D. Christodoulides, and U. Peschel, Observation of Bloch oscillations in complex PT-symmetric photonic lattices, Sci. Rep. **5**, 17760 (2015).

[31] Z. Zhang, Y. Zhang, J. Sheng, L. Yang, M.-A. Miri, D. N. Christodoulides, B. He, Y. Zhang, and M. Xiao, Observation of parity-time symmetry in optically induced atomic lattices, Phys. Rev. Lett. **117**, 123601 (2016).

[32] P. Peng, W. Cao, C. Shen, W. Qu, J. Wen, L. Jiang, and Y. Xiao, Anti-parity-time symmetry with flying atoms, Nat. Phys. **12**, 1139 (2016).

[33] F. Monticone, C. A. Valagiannopoulos, and A. Alù, Aberration-free imaging based on parity-time symmetric nonlocal metasurfaces, Phys. Rev. X **6**, 041018 (2016).

[34] T. E. Lee, Anomalous edge state in a non-Hermitian lattice, Phys. Rev. Lett. **116**, 133903 (2016).

[35] Y. Xiong, Why does bulk boundary correspondence fail in some non-Hermitian topological models, J. Phys. Commun. **2**, 035043 (2018).

[36] V. M. Martinez Alvarez, J. E. Barrios Vargas, and L. E. F. Foa Torres, Non-Hermitian robust edge states in one dimension: Anomalous localization and eigenspace condensation at exceptional points, Phys. Rev. B **97**, 121401(R) (2018).

[37] S. Yao and Z. Wang, Edge states and topological invari ants of non-Hermitian systems, Phys. Rev. Lett. **121**, 086803 (2018).

[38] F. K. Kunst, E. Edvardsson, J. C. Budich, and E. J. Bergholtz, Biorthogonal bulk-boundary correspondence in non-Hermitian systems, Phys. Rev. Lett. **121**, 026808 (2018).

[39] C. Yin, H. Jiang, L. Li, R. Lü, and S. Chen, Geometrical meaning of winding number and its characterization of topological phases in one-dimensional chiral non-Hermitian systems, Phys. Rev. A **97**, 052115 (2018).

[40] F. Song, S. Yao, and Z. Wang, Non-Hermitian skin effect and chiral damping in open quantum systems, Phys. Rev. Lett. **123**, 170401 (2019).

[41] A. Ghatak and T. Das, New topological invariants in non-Hermitian systems, J. Phys.: Condens. Matter **31**, 263001 (2019).

[42] C. H. Lee and R. Thomale, Anatomy of skin modes and topology in non-Hermitian systems, Phys. Rev. B **99**, 201103(R) (2019).

[43] K. Yokomizo and S. Murakami, Non-Bloch band theory of non-Hermitian systems, Phys. Rev. Lett. **123**, 066404 (2019).

[44] S. Longhi, Probing non-Hermitian skin effect and non-Bloch phase transitions, Phys. Rev. Res. **1**, 023013 (2019).

[45] E. Edvardsson, F. K. Kunst, and E. J. Bergholtz, Non Hermitian extensions of higher-order topological phases and their biorthogonal bulk-boundary correspondence, Phys. Rev. B **99**, 081302(R) (2019).

[46] D. S. Borgnia, A. J. Kruchkov, and R. J. Slager, Non-Hermitian boundary modes and topology, Phys. Rev. Lett. **124**, 056802 (2020).

[47] Y. Yi and Z. Yang, Non-Hermitian skin modes induced by on-site dissipations and chiral tunneling effect, Phys. Rev. Lett. **125**, 186802 (2020).

[48] K. Kawabata, M. Sato, and K. Shiozaki, Higher-order non-Hermitian skin effect, Phys. Rev. B **102**, 205118 (2020).

[49] L. Li, C. H. Lee, and J. Gong, Topological switch for non-Hermitian skin effect in cold-atom systems with loss, Phys. Rev. Lett. **124**, 250402 (2020).

[50] C. X. Guo, C. H. Liu, X. M. Zhao, Y. Liu, and S. Chen, Exact solution of non-Hermitian systems with generalized boundary conditions: Size-dependent boundary effect and fragility of the skin effect, Phys. Rev. Lett. **127**, 116801 (2021).

[51] N. Okuma and M. Sato, Non-Hermitian skin effects in hermitian correlated or disordered systems: Quantities sensitive or insensitive to boundary effects and pseudo-quantum-number, Phys. Rev. Lett. **126**, 176601 (2021).

[52] F. Roccati, Non-Hermitian skin effect as an impurity problem, Phys. Rev. A **104**, 022215 (2021).

[53] X. Zhang, Y. Tian, J.-H. Jiang, M.-H. Lu, and Y.-F. Chen, Observation of higher-order non-Hermitian skin effect, Nat. Commun. **12**, 5377 (2021).

[54] H. Zhang, T. Chen, L. Li, C. H. Lee, and X. Zhang, Electrical circuit realization of topological switching for the non-Hermitian skin effect, Phys. Rev. B **107**, 085426 (2023).

[55] R. Lin, Tommy Tai, L. Li, and C. H. Lee, Topological non-Hermitian skin effect, Front. Phys. **18**, 53605 (2023).

[56] K. Yokomizo and S. Murakami, Non-Bloch bands in two dimensional non-Hermitian systems, Phys. Rev. B **107**, 195112 (2023).

[57] Z. Ou, Y. Wang, and L. Li, Non-Hermitian boundary spectral winding, Phys. Rev. B **107**, L161404 (2023).

[58] X. Ma, K. Cao, X. Wang, Z. Wei, and S. Kou, Non-Hermitian chiral skin effect, Phys. Rev. Res. **6**, 013213 (2024).

[59] D. C. Brody, Biorthogonal quantum mechanics, J. Phys. A: Math. Theor. **47**, 035305 (2014).

[60] G.-P. Zheng and G.-T. Wang, Time evolution of non-Hermitian systems driven by a high-frequency field, Int. J. Theor. Phys. **61**, 38 (2022).

[61] A. U. Hassan, G. L. Galmiche, G. Harari, P. LiKamWa, M. Khajavikhan, M. Segev, and D. N. Christodoulides, Chiral state conversion without encircling an exceptional point, Phys. Rev. A **96**, 052129 (2017).

[62] Q. Liu, J. Liu, D. Zhao, and B. Wang, On-chip experiment for chiral mode transfer without enclosing an exceptional point, Phys. Rev. A **103**, 023531 (2021).

[63] F. Yu, X.-L. Zhang, Z.-N. Tian, Q.-D. Chen, and H.-B. Sun, General rules governing the dynamical encircling of an arbitrary number of exceptional points, Phys. Rev. Lett. **127**, 253901 (2021).

[64] H. Nasari, G. Lopez-Galmiche, H. E. Lopez-Aviles, A. Schumer, A. U. Hassan, Q. Zhong, S. Rotter, P. LiKamWa, D. N. Christodoulides, and M. Khajavikhan, Observation of chiral state transfer without encircling an exceptional point, Nature (London) **605**, 256 (2022).

[65] T. Kato, *Perturbation Theory for Linear Operators* (Springer, Berlin, 1966).

[66] H. Cartarius, J. Main, and G. Wunner, Exceptional points in atomic spectra, Phys. Rev. Lett. **99**, 173003 (2007).

[67] M. V. Berry and R. Uzdin, Slow non-Hermitian cycling: exact solutions and the Stokes phenomenon, J. Phys. A: Math. Theor. **44**, 435303 (2011).

[68] R. Uzdin, A. Mailybaev, and N. Moiseyev, On the observability and asymmetry of adiabatic state flips generated by exceptional points, J. Phys. A: Math. Theor. **44**, 435302 (2011).

[69] I. Gilary and N. Moiseyev, Asymmetric effect of slowly varying chirped laser pulses on the adiabatic state exchange of a molecule, J. Phys. B: At., Mol. Opt. Phys. **45**, 051002 (2012).

[70] I. Gilary, A. A. Mailybaev, and N. Moiseyev, Time-asymmetric quantum-state-exchange mechanism, Phys. Rev. A **88**, 010102(R) (2013).

[71] T. J. Milburn, J. Doppler, C. A. Holmes, S. Portolan, S. Rotter, and P. Rabl, General description of quasiadiabatic dynamical phenomena near exceptional points, Phys. Rev. A **92**, 052124 (2015).

[72] J. Doppler, A. A. Mailybaev, J. Bohm, U. Kuhl, A. Girschik, F. Libisch, T. J. Milburn, P. Rabl, N. Moiseyev, and S. Rotter, Dynamically encircling an exceptional point for asymmetric mode switching, Nature (London) **537**, 76 (2016).

[73] A. U. Hassan, B. Zhen, M. Soljačić, M. Khajavikhan, and D. N. Christodoulides, Dynamically encircling exceptional points: Exact evolution and polarization state conversion, Phys. Rev. Lett. **118**, 093002 (2017).

[74] S. Longhi, Floquet exceptional points and chirality in non-Hermitian Hamiltonians, J. Phys. A: Math. Theor. **50**, 505201 (2017).

[75] J. W. Yoon, Y. Choi, C. Hahn, G. Kim, S. H. Song, K.-Y. Yang, J. Y. Lee, Y. Kim, C. S. Lee, J. K. Shin, H.-S. Lee, and P. Berini, Time-asymmetric loop around an exceptional point over the full optical communications band, Nature (London) **562**, 86 (2018).

[76] X.-L. Zhang, S. Wang, B. Hou, and C. T. Chan, Dynamically encircling exceptional points: *In situ* control of encircling loops and the role of the starting point, Phys. Rev. X **8**, 021066 (2018).

[77] X. L. Zhang, T. Jiang, and C. T. Chan, Dynamically encircling an exceptional point in anti-parity-time symmetric systems: Asymmetric mode switching for symmetry-broken modes, Light: Sci. Appl. **8**, 88 (2019).

[78] C. Yuce, State conversions around exceptional points, J. Phys. A: Math. Theor. **52**, 485301 (2019).

[79] M.-A. Miri and A. Alù, Exceptional points in optics and photonics, Science **363**, eaar7709 (2019).

[80] Q. Liu, S. Li, B. Wang, S. Ke, C. Qin, K. Wang, W. Liu, D. Gao, P. Berini, and P. Lu, Efficient mode transfer on a compact silicon chip by encircling moving exceptional points, Phys. Rev. Lett. **124**, 153903 (2020).

[81] A. Li, J. Dong, J. Wang, Z. Cheng, J. S. Ho, D. Zhang, J. Wen, X. L. Zhang, C. T. Chan, A. Alù, C. W. Qiu, and L. Chen, Hamiltonian hopping for efficient chiral mode switching in encircling exceptional points, Phys. Rev. Lett. **125**, 187403 (2020).

[82] J. Höller, N. Read, and J. G. E. Harris, Non-Hermitian adiabatic transport in spaces of exceptional points, Phys. Rev. A **102**, 032216 (2020).

[83] W. Liu, Y. Wu, C.-K. Duan, X. Rong, and J. Du, Dynamically encircling an exceptional point in a real quantum system, Phys. Rev. Lett. **126**, 170506 (2021).

[84] L. Geng, W. Zhang, X. Zhang, and X. Zhou, Topological mode switching in modulated structures with dynamic encircling of an exceptional point, Proc. R. Soc. A **477**, 20200766 (2021).

[85] C. F. Fong, Y. Ota, Y. Arakawa, S. Iwamoto, and Y. K. Kato, Chiral modes near exceptional points in symmetry broken H1 photonic crystal cavities, Phys. Rev. Res. **3**, 043096 (2021).

[86] H. Hu, S. Sun, and S. Chen, Knot topology of exceptional point and non-Hermitian no-go theorem, Phys. Rev. Res. **4**, L022064 (2022).

[87] N. S. Nye, Universal state conversion in discrete and slowly varying non-Hermitian cyclic systems: An analytic proof and exactly solvable examples, Phys. Rev. Res. **5**, 033053 (2023).

[88] C. Hang, G. Huang, and V. V. Konotop, $\mathcal{PT}$ symmetry with a system of three-level atoms, Phys. Rev. Lett. **110**, 083604 (2013).

[89] H. Menke, M. Klett, H. Cartarius, J. Main, and G. Wunner, State flip at exceptional points in atomic spectra, Phys. Rev. A **93**, 013401 (2016).

[90] W. D. Heiss and G. Wunner, Chiral behaviour of the wave functions for three wave guides in the vicinity of an exceptional point of third order, Eur. Phys. J. D **71**, 312 (2017).

[91] L. Guo, L. Du, C. Yin, Y. Zhang, and S. Chen, Dynamical evolutions in non-Hermitian triple-well systems with a complex potential, Phys. Rev. A **97**, 032109 (2018).

[92] X.-L. Zhang and C. T. Chan, Dynamically encircling exceptional points in a three-mode waveguide system, Commun. Phys. **2**, 63 (2019).

[93] W. Tang, K. Ding, and G. Ma, Experimental realization of non-Abelian permutations in a three-state non-Hermitian system, Natl. Sci. Rev. **9**, nwac010 (2022).

[94] H. P. Breuer and F. Petruccione, *The Theory of Open Quantum Systems* (Oxford University Press, Oxford, UK, 2006).

[95] G. Lindblad, On the generators of quantum dynamical semigroups, Commun. Math. Phys. **48**, 119 (1976).

[96] V. Gorini, A. Kossakowski, and E. C. G. Sudarshan, Completely positive dynamical semigroups of N-level systems, J. Math. Phys. **17**, 821 (1976).